

Dynamics of Bloch vectors and the channel capacity of a non identical charged qubit pair

N. Metwally, M. Abdel-Aty and A.-S. F. Obada*

Mathematics Department, College of Science, Bahrain University, 32038 Bahrain

*Mathematics Department, Faculty of Science, Al-Azhar University, Cairo, Egypt

We have considered a system of two superconducting charge qubits capacitively coupled to a microwave resonator. The dynamics of the Bloch vectors are investigated for different regimes. By means of the Bloch vectors and cross dyadic we quantify the degree of entanglement contained in the generated entangled state. We consider different values of the system parameters to discuss the dynamics of the channel capacity between the qubits. We show that there is an important role played by initial state settings, coupling constant and the mean photon number on generating entangled state with high degree of entanglement and high capacity

Keywords: Charged Qubit, Bloch vectors Entanglement, Capacity .

1 Introduction

Quantum entanglement is a quantum mechanical phenomenon in which the quantum states of two or more objects have to be described with reference to each other, even though the individual objects may be spatially separated. It is an essential component in many quantum information processing applications, such as quantum computation [1], teleportation [3] and cryptography [2] and dense coding [4, 5]. Therefore, it is essential to create and manipulate entangled states for quantum information tasks. The basic element of the quantum information is the quantum bit (qubit) which is considered as a two level system. Consequently, most of the research concentrate to generate entanglement between two level systems. Among these systems, superconducting charged qubits i.e. the Cooper pair box [6, 12].

In the last years the generated entangled states between Cooper pairs has been received a lot of attenuation. This is due to its properties as a two-level quantum system, which makes it a candidate as a qubit in a quantum computer [7, 8]. Also, recently these types of charged particles has been used to implement a Shor's factorization [9], Deutsch-Jozsa algorithm [10], the Grover search algorithm protocol [11], and the quantum computing with a single molecular ensemble. On the other hand theses charged pairs have been used to realize a controlled phase gate [13]. All these

applications have encouraged different authors to study the entangled properties of these systems. As an example, the entanglement between two superconducting qubits has been generated by the interaction with nonclassical radiation [14]. Rodrigues et al. have evaluated the entanglement of superconducting charge qubits by homodyne measurement [15, 16]. The entropy squeezing and the emission spectra of a single-cooper pair have been investigated [17].

On the other hand, it is known that the Bloch vector gives one of the possible descriptions of N-level quantum states, because it is defined as a vector whose components are expectation values of some observables. So, we can use it to describe the density operator of any system [18]. These vectors (called coherent vectors), play a central role in quantifying the degree of entanglement, where Englert [19] has used it to evaluate the entanglement dyadic which represent a measure of the degree of entanglement. Addressing this issue with Cooper pair box systems is the main aim of the present paper.

In this article we propose to study a system of two-Cooper pairs interacting with a single cavity mode. We investigate the dynamics of the polarized vector for each individual qubit and the channel capacity of the entangled Cooper pair for different values of the system parameters. This paper is organized as follows. In section 2, we introduce our model and its solution. We devote section 3, to investigate the relation between the Bloch vectors and the quantum entanglement. In section 4, we investigate the effect of the structure of the initial state and the mean photon number on the transmission rate of information between two parties via the channel capacity. Finally, we end up with our conclusion.

2 Model and its solution

Our system consists of two superconducting charge qubits each coupled capacitively to a strapline resonator. Each charged qubit consists of a small superconducting island with a Cooper pair charge Q . This island connected by two identical Josephson junctions, with capacity C_j and Josephson coupling energy E_j , to a superconducting electrode. This system can be describe as a pair of two-level systems coupled to a simple harmonic oscillator. The charging energy of the qubits and their coupling to the resonator can be controlled by the application of magnetic and electric fields. By using the a rotating wave approximation, the system can be described by the

Hamiltonian [15].

$$H = \hbar\omega(a^\dagger a + \frac{1}{2}) + (E_1\sigma_z + E_2\tau_z) + \hbar \sum_{i=1}^2 \lambda_i(a\sigma_i^+ + a^\dagger\sigma_i^-), \quad (1)$$

where $\sigma_z = |e\rangle_1\langle e| - |g\rangle_1\langle g|$ for the first qubit, $\tau_z = |e\rangle_2\langle e| - |g\rangle_2\langle g|$ for the second qubit, a^\dagger and a are the creation and annihilation operators of photons with frequency ω , $E_{1,2}$ are the charging energies of the qubits, and $\lambda_{1,2}$ are the resonator-qubit coupling terms.

Our target of this section is to derive the time-dependent density matrix which enables us to discuss the statistical properties of the present model. For this reason let us assume that the initial state of the two charged qubits are prepared in a superposition state which can be written as $|\psi_c(0)\rangle = a|ee\rangle + b|gg\rangle$, $|a|^2 + |b|^2 = 1$, while the cavity field starts from a coherent state, $|\psi_f(0)\rangle = \sum_{n=0}^{\infty} q_n|n\rangle$, $q_n = \frac{\alpha^n}{\sqrt{n!}} \exp(-\frac{1}{2}|\alpha|^2)$. Now we can write the time evolution of the density operator in the form

$$\rho(t) = \mathcal{U}(t)\rho(0)\mathcal{U}^\dagger(t), \quad (2)$$

where $\mathcal{U}(t) = \exp(-iHt/\hbar)$ is the time-dependent unitary operator and $\rho(0) = |\psi(0)\rangle\langle\psi(0)|$. Since the invariant sub-space of the global system can be considered as a set of complete basis of the atom-field. Since, we are interested in the contribution of the Bloch vector in quantifying the degree of entanglement, we express the density operator $\rho_c(t)$ of the system charged system by means of the Bloch vector for each qubit and the cross dyadic. After tracing out the state of the field one gets the state of the charged qubit as,

$$\rho_c(t) = \frac{1}{4}(1 + \vec{s} \cdot \sigma^\downarrow + \vec{t} \cdot \tau^\downarrow + \vec{\sigma} \cdot \overleftrightarrow{C} \cdot \tau^\downarrow), \quad (3)$$

where $\sigma^\downarrow = (\sigma_x, \sigma_y, \sigma_z)$, $\tau^\downarrow = (\tau_x, \tau_y, \tau_z)$ are the Pauli matrices for the first and second qubit respectively, while $\vec{s} = (s_x, s_y, s_z)$, $\vec{t} = (t_x, t_y, t_z)$ and are the Bloch vectors for the first and the second qubits and \overleftrightarrow{C} is the cross dyadic, are defined as follows:

$$\begin{aligned} s_x(t) &= A_{n+1}(t)c_n^*(t) + B_{n+1}(t)D_n^*(t) + C_n(t)A_{n+1}^*(t) + D_n(t)B_{n+1}^*(t), \\ s_y(t) &= i[-A_{n+1}(t)C_n^*(t) - B_{n+1}(t)D_n^*(t) + C_n(t)A_{n+1}^*(t) + D_n(t)B_{n+1}^*(t)], \\ s_z(t) &= |A_n(t)|^2 + |B_n(t)|^2 - |C_n(t)|^2 - |D_n(t)|^2, \end{aligned} \quad (4)$$

while for the second qubit,

$$\begin{aligned}
t_x(t) &= A_{n+1}(t)B_n^*(t) + B_n(t)A_{n+1}^*(t) + C_{n+1}(t)D_n^*(t) + D_n(t)C_{n+1}^*(t), \\
t_y(t) &= i \left[-A_{n+1}(t)B_n^*(t) + B_n(t)A_{n+1}^*(t) - C_{n+1}(t)D_n^*(t) + D_n(t)C_{n+1}^*(t) \right], \\
t_z(t) &= |A_n(t)|^2 - |B_n(t)|^2 + |C_n(t)|^2 - |D_n(t)|^2,
\end{aligned} \tag{5}$$

In addition to the elements of the cross dyadic, $\overleftrightarrow{\mathbb{C}}$

$$\begin{aligned}
c_{xx} &= A_{n+2}(t)D_n^*(t) + B_n(t)C_n^*(t) + C_n(t)B_n^*(t) + D_n(t)A_{n+2}^*(t), \\
c_{xy} &= i \left[-A_{n+2}(t)D_n^*(t) + B_n(t)C_n^*(t) - C_n(t)B_n^*(t) + D_n(t)A_{n+2}^*(t) \right], \\
c_{xz} &= A_{n+1}(t)C_n^*(t) - B_{n+1}(t)D_n^*(t) + C_n(t)A_{n+1}^*(t) - D_n(t)B_{n+1}^*(t) \\
c_{yx} &= i \left[-A_{n+2}(t)D_n^*(t) - B_n(t)C_n^*(t) + C_n(t)B_n^*(t) + D_n(t)A_{n+2}^*(t) \right], \\
c_{yy} &= -A_{n+2}(t)D_n^*(t) + B_n(t)C_n^*(t) + C_n(t)B_n^*(t) - D_n(t)A_{n+2}^*(t), \\
c_{yz} &= i \left[-A_{n+1}(t)C_n^*(t) + B_{n+1}(t)D_n^*(t) + C_n(t)A_{n+1}^*(t) - D_n(t)B_{n+1}^*(t) \right], \\
c_{zx} &= A_{n+1}(t)B_n^*(t) + B_n(t)A_{n+1}^*(t) - C_{n+1}(t)D_n^*(t) - D_n(t)C_{n+1}^*(t), \\
c_{zy} &= i \left[-A_{n+1}(t)B_n^*(t) + B_n(t)A_{n+1}^*(t) - C_{n+1}(t)D_n^*(t) + D_n(t)C_{n+1}^*(t) \right] \\
c_{zz} &= |A_n(t)|^2 - |B_n(t)|^2 - |C_n(t)|^2 + |D_n(t)|^2,
\end{aligned} \tag{6}$$

where,

$$\begin{aligned}
A_n(t) &= \sum_n^{\infty} \left\{ \frac{-a}{\mu_n - \nu_n} \left((1 + R^2)\beta_n^2 (\cos t\sqrt{\mu_n} - \cos(t\sqrt{\nu_n})) + \mu_n \cos(t\sqrt{\mu_n}) + \nu_n \cos(t\sqrt{\nu_n}) \right) \right. \\
&\quad \left. + \frac{2b\beta_n\gamma_n}{\mu_n - \nu_n} (\cos(t\sqrt{\mu_n}) - \cos(t\sqrt{\nu_n})) \right\}, \\
B_n(t) &= \sum_n^{\infty} \left\{ \frac{-iaR\gamma_n}{\mu_n - \nu_n} \left(\frac{(1 - R^2)\beta_n^2 + \mu_n}{\sqrt{\mu_n}} \sin(t\sqrt{\mu_n}) + \frac{(1 - R^2)\beta_n^2 - \nu_n}{\sqrt{\nu_n}} \sin(t\sqrt{\nu_n}) \right) \right. \\
&\quad \left. + \frac{ib\beta_n}{\mu_n - \nu_n} \left(((1 - R^2)\gamma_n^2 - \mu_n) \sin(t\sqrt{\mu_n}) - ((1 - R^2)\gamma_n^2 - \nu_n) \sin(t\sqrt{\nu_n}) \right) \right\}, \\
C_n(t) &= \sum_{n=0}^{\infty} \left\{ \frac{ia\gamma_n}{\mu_n - \nu_n} \left(\frac{(1 - R^2)\beta_n^2 - \mu_n}{\sqrt{\mu_n}} \sin(t\sqrt{\mu_n}) - \frac{(1 - R^2)\beta_n^2 - \nu_n}{\sqrt{\nu_n}} \sin(t\sqrt{\nu_n}) \right) \right. \\
&\quad \left. - \frac{ibR\beta_n}{\mu_n - \nu_n} \left(\frac{(1 - R^2)\gamma_n^2 + \mu_n}{\sqrt{\mu_n}} \sin(t\sqrt{\mu_n}) + \frac{(1 - R^2)\gamma_n^2 - \nu_n}{\sqrt{\nu_n}} \sin(t\sqrt{\nu_n}) \right) \right\}, \\
D_n(t) &= \sum_{n=0}^{\infty} \left\{ -\frac{b}{\mu_n - \nu_n} \left((1 + R^2)\gamma_n^2 (\cos(t\sqrt{\mu_n}) - \cos(t\sqrt{\nu_n})) + \mu_n \cos(t\sqrt{\mu_n}) + \nu_n \cos(t\sqrt{\nu_n}) \right) \right. \\
&\quad \left. + \frac{2a\beta_n\gamma_n}{\mu_n - \nu_n} (\cos(t\sqrt{\mu_n}) - \cos(t\sqrt{\nu_n})) \right\},
\end{aligned} \tag{7}$$

and, $\gamma_n = \sqrt{1+n}$, $\beta_n = \sqrt{n+2}$, $\mu_n = \frac{1}{2}(\delta_n + \sqrt{\delta_n^2 - 4\Delta_n^2})$, $\nu_n = \frac{1}{2}(\delta_n - \sqrt{\delta_n^2 - 4\Delta_n^2})$, $\delta_n = (1 + R^2)(\gamma_n^2 + \beta_n^2)$, $\Delta_n = (1 - R^2)^2\beta_n^2\gamma_n^2$ and $R = \frac{\lambda_2}{\lambda_1}$

3 Dynamics of Bloch Vectors

In this section, taking into account the possible extension of the methods which will be discussed in this work to higher-dimensional situations and to mixed states, the present strategy will certainly need to be modified and integrated by developing more sophisticated tools, including the use of multiple operations to yield properly defined entanglement and generalizations to mixed-states cases. At this end, we can say that, the qubit $|\psi\rangle = a|0\rangle + b|1\rangle$, can be represented as a point (θ, ϕ) on a unit sphere called the Bloch sphere. Define the angles θ and ϕ by letting $a = \cos(\frac{\theta}{2})$ and $b = e^{i\phi} \sin(\frac{\theta}{2})$, then $|\psi\rangle$ is represented by the unit vector $(\cos \phi \sin \theta, \sin \phi \sin \theta, \cos \theta)$ called Bloch vector.

Here, we investigate the dynamics of the Bloch vectors (Polarized vector), for different values of the mean photon number \bar{n} , the relative coupling R and different classes of the initial state of the charged system. In Fig. (1), we assume that the charged qubits are prepared in the excited state $\rho_e(0) = |ee\rangle\langle ee|$ and the mean photon number $\bar{n} = 20$, while the relative coupling $R = \lambda_2/\lambda_1$ takes different values. In Fig. (1a), we consider a small value of R , which means that the coupling between the second qubit and the cavity field is very weak. It is clear that, the Bloch vector for the second qubit is bigger than the Bloch vector for the first qubit. This is due to the weak coupling between the second qubit and the cavity field. So, the chance that the second qubit interacts with the field is very small. On the other hand, as soon as the interaction goes on, we can see that the Bloch vector for the first qubit decreases rapidly. This is due to the strong coupling between the first charged qubit and the cavity mode. So for this situation, there is an entangled state generated between the first qubit and the field, while the second qubit is almost factorized. This phenomenon is not observed in Fig. (1b), where we consider large values of the coupling R . For the numerical values we consider $R = 0.9$, i.e $\lambda_1 \simeq \lambda_2$. In this case the two Bloch vectors increase and decrease together. This means that the probability that both qubits interact with the field is almost the same. Also, we can notice that, this choice causes a shrink of the Bloch vectors, where the maximum values almost 0.6.

It is interesting to mention to the fact that, the maximum entangled state as

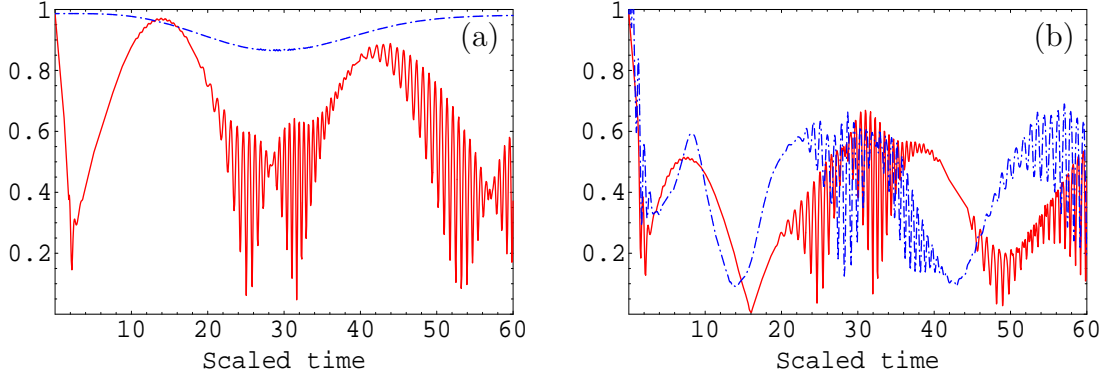


Figure 1: The Bloch vectors as functions of the scaled time. The two-qubit system is prepared initially in an excited state $|e_1, e_2\rangle$, and the field starts from a coherent state with a mean-photon number $\bar{n} = 20$. The solid curves for the first qubit while the dot curves for the second qubit. The relative coupling is (a) for $R = 0.003$ (b) $R = 0.9$.

Bell states has zero Bloch vectors. So, as the Bloch vectors decrease, the possibility for obtaining an entangled state with high degree of entanglement increases. So, by using a suitable values of the coupling constant, one can control the Bloch vectors and consequently it is possible to generate an entangled state with high degree of entanglement. In Fig. (2), we plot the Bloch sphere, with radius equal 0.4 units, at specific time in the interval $[10.2 - 11.6]$, where we consider that the charged qubits are prepared in the excited state and $R = 0.9$. The amplitude and the direction of the Bloch vector for the first qubit are shown. One can see that at $t = 10.2$, the Bloch vector parallel to y -axis and it has a large value. As the time increases (say $t = 10.3, 10.4$), the Bloch vector inside the sphere and it could great or equal 0.4. As the time increases further, the Bloch vector appears in a different direction and its amplitude shrinks, this is shown for $t = 10.5$. As time increases more the length of the Bloch vector increases and its direction change.

In Fig. (3), we assume that the charged system is prepared in the partially entangled state $a|ee\rangle + b|gg\rangle$. For small values for the relative coupling the general behavior of the two vectors is somehow similar with small differences. Comparing Figs.(1a) and (2a), we see that the minimum point of the Bloch vector is decreased for the partial entangled state, which means that, using this class of the initial state, it will be more efficient to generate entangled state with high degree of entanglement. For large values of the relative coupling constant, $R = 0.9$, the behavior of the two

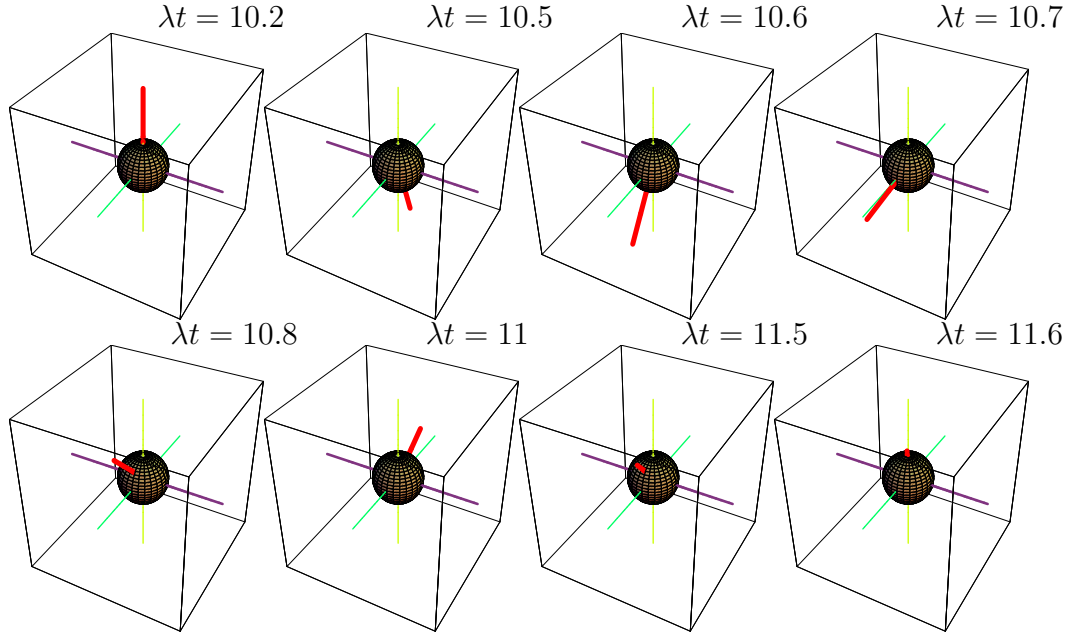


Figure 2: The Bloch sphere for a charged system prepared initially in an excited state with $\bar{n} = 20, R = 0.9$. The thick line represents the length of the Bloch vector for the first qubits.

Bloch vectors are similar. For a specific time one of the Bloch vectors reaches to zero, in this case there is a maximum entangled state generated between the two charged qubit,

In Fig. (3c), we consider the mean photon number $\bar{n} = 10$ and R is small. In this case, we can see that the minimum point of the Bloch vectors is very small compared with that depicted in Fig. (3a). Also, the Bloch vector for the second qubit is shrunk more for small values of the mean photon number. This phenomena is clearly appeared in Fig. (3d), where we consider a large value of the coupling constant. In additional to the coincidence of the behavior of the Bloch vector for the two qubits, the two vectors are shrinking more. So, in this case the possibility of generating entangled state with high degree of entanglement is increased.

4 Degree of Entanglement

To quantify the degree of entanglement between the two charged qubits, we use a measure which is defined by means of the Bloch vectors and the cross dyadic. We

define the entangled dyadic as

$$\overleftrightarrow{E} = \overleftrightarrow{C} - s\overleftrightarrow{t} \quad (8)$$

where \overleftrightarrow{C} is a 3×3 matrix which is defined by (6) and $s\overleftrightarrow{t}$ is also 3×3 matrix whose elements can be obtained from (4) and (5). The degree of entanglement is defined by

$$DoE = tr\{\overleftrightarrow{E}^T \cdot \overleftrightarrow{E}\} \quad (9)$$

where \overleftrightarrow{E}^T is the transpose matrix of the dyadic \overleftrightarrow{E}

The amount of entanglement between the entangled charged qubits is shown in Fig. 4, in which we consider different regimes. In the first regime, we assume that the two qubits are prepared initially in the following excited state $|\psi(0)\rangle_c = |ee\rangle$ while the field starts from a coherent state with a mean photon number $\bar{n} = 20$. In Fig. (4a), we see that for a small value of the coupling constant (say $R = 0.003$), there is no any quantum correlation between the two charged qubit expect on the interval $[19.2-40.5]$, where in this interval the Bloch of the second qubit decreases.

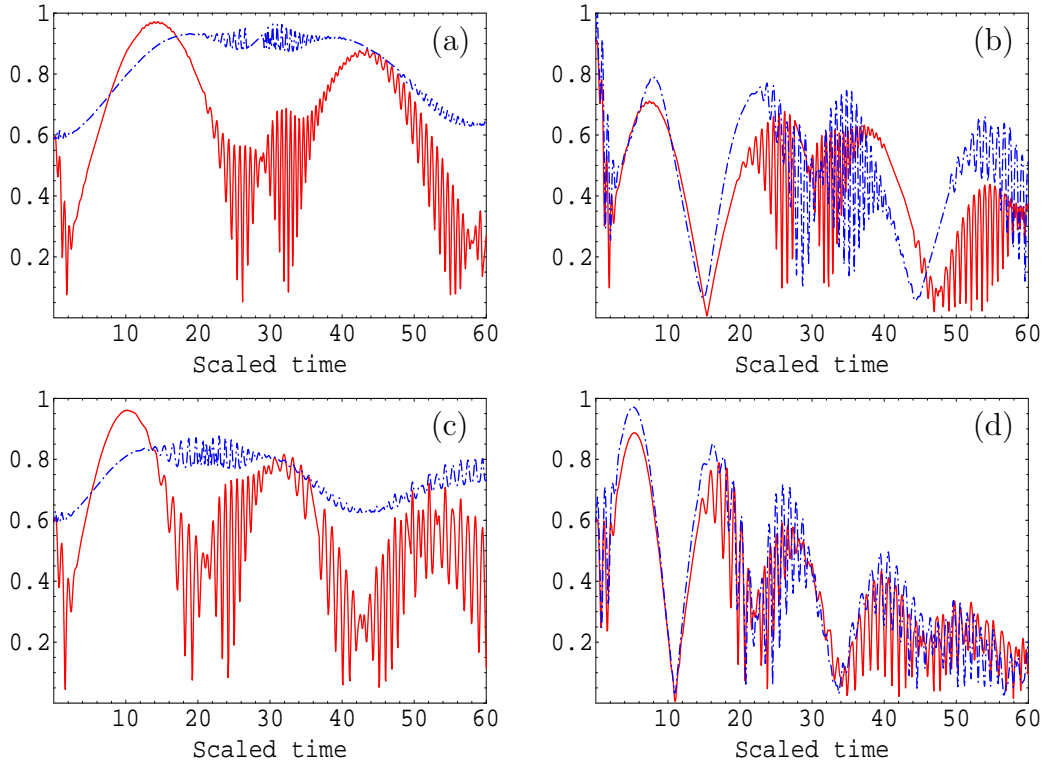


Figure 3: The same as Fig.(1) but the charged qubits are prepared initially a partial entangled state.

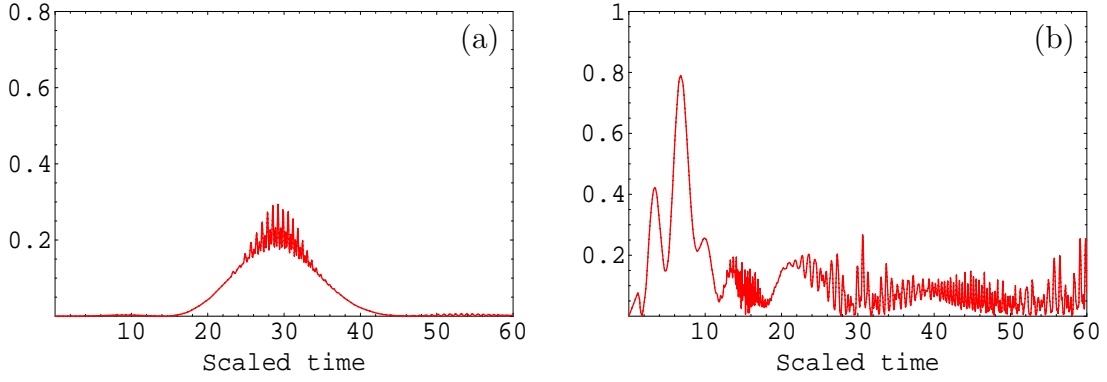


Figure 4: The degree of entanglement for a charged system prepared initially in an excited state with $\bar{n} = 20$. (a) For $R = 0.003$ (a) excited (b) $R = 0.9$.

This means that in this intervals, the three subsystems (the two charged qubits and the field) interact with each others. Also, from this figure, we can see that the maximum amount of entanglement is obtained at the minimum point of the Bloch vectors of both qubits. This phenomena, also, is shown in Fig. (4b), where we consider $R = 0.9$. As soon as the interaction starts, (scaled time is greater than zero), the entangled state starts to be generated. It is obvious to realize that the development of the entanglement depends on the dynamics of the Bloch vectors.

The effect of different setting of the initial state of the charged qubit is seen in Fig.(5), where we assume that the system is prepared initially in a partially entangled state. Fig. (5a), is devoted to consider a weak correlation case (say $R = 0.003$).

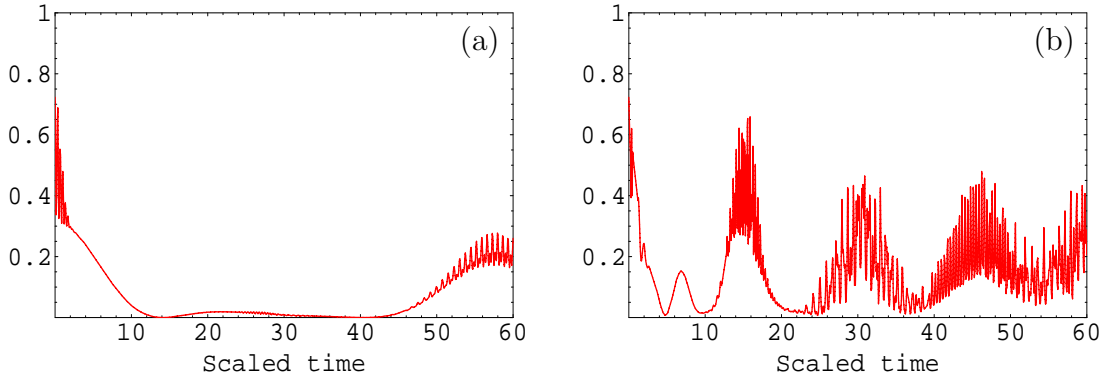


Figure 5: The degree of entanglement for a charged system prepared initially in partially entangled states with $\bar{n} = 20$. (a) For $R = 0.003$ (a) excited (b) $R = 0.9$.

From this figure it is clear that the degree of entanglement decreases with time until it reaches a minimum point at $\lambda_1 t \simeq 15$. From Fig. (3a), we see that the Bloch vector for both qubit are maximum and consequently the degree of entanglement will be minimum according to the definition (9). In the interval $[40 - 60]$, the degree of entanglement starts to increase another time, where in this interval of time the Bloch vector decrease (see Fig. (3a)). For a strong correlation the dynamics is seen in Fig. (5b). It is clear that the degree of entanglement is much stronger, where the efficiency of generating entangled state in this case is much higher. Also, the evolvment of the degree of entanglement depends on the evolvment of the Bloch vector for each qubit.

In this context it is very important to investigate the evolvment of the degree of entanglement for different values of the mean photon number \bar{n} . We choose the case for the weak coupling, where $R = 0.003$. In Fig.(6a), we assume that the system has been processed in advance in an excites state. The usual effect of the mean photon number is seen where the Rabi oscillation is shifted to the left. In this case the maximum amount of entanglement is smaller than that depicted for $\bar{n} = 20$ (Fig. (4a)). But on the other hand, there is an entangled state is generated in the interval $[50 - 60]$, while on the corresponding interval the charged system behaves as a product state. In Fig. (6b), we plot the degree of entanglement for a charged qubit is prepared in partially entangled state. In this case the degree of entanglement is much better than that shown in Fig. (5a), where $\bar{n} = 20$. So, For the weak interaction one can generate an entangled state between the two charged qubits by reducing the number of photons in the cavity mode.

5 The channel Capacity

In this section we investigate the effect of the structure of the initial state and the mean photon number on the transmission rate of information from a sender (Alice), to a receiver (Bob). This task can be performed by employing the dense coding protocol [3], [20, 21]. The main idea of this protocol is that, Alice and Bob share an entangled qubit pair. They used it as a channel, where Alice can encode two classical bits in her qubit by using local operation. Alice sends her qubit to Bob, who will try to decode the information. The amount of information gained by Bob depends on the capacity of the channel. In this context, we try to show how the capacity of the channel and hence the rate of transmit information depend on the

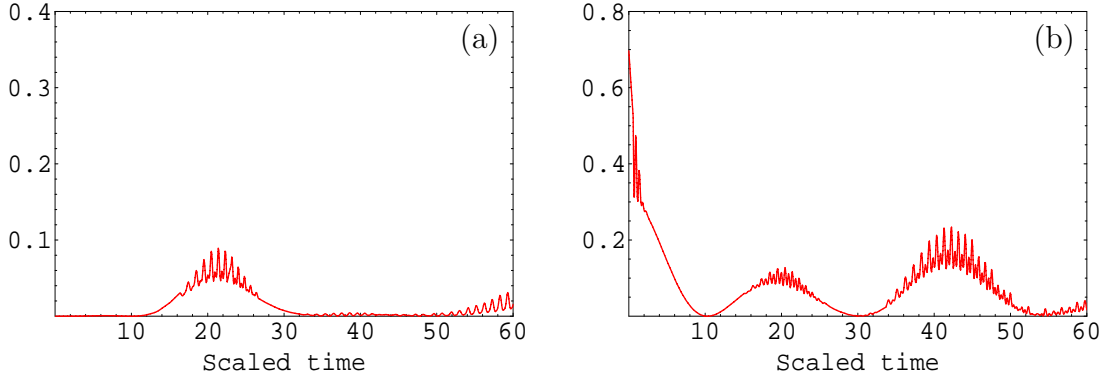


Figure 6: The degree of entanglement for a charged system prepared initially in partially entangled states with $\bar{n} = 10$, $R = 0.003$. For (a) excited (b) partially entangled state.

structure of the initial states, the relative coupling and the mean photon number. For $N \times M$ state system, the dense coding capacity is given by

$$\mathcal{C} = \log D_A + \mathcal{S}(\rho_B) - \mathcal{S}(\rho_{AB}), \quad (10)$$

where $D_A = N$, $\rho_B = \text{tr}_A\{\rho_{AB}\}$ and $\mathcal{S}(\cdot)$ is the Von Numann entropy. Since we consider entangled two qubits, then our system is in 2×2 dimension. Fig. 5, shows the behavior of the capacity of the entangled quantum channel, where we consider the two charged qubits are in excited state. We investigate the effect of the coupling constant, the mean photon number and the setting of the initial state of the charged system. Fig. (7a), shows the behavior of the channel capacity for a charged system with a strong coupling with the field, where we assume that $R = 0.9$ and the mean photon number $\bar{n} = 10$. From this figure it is clear that the channel capacity for a charged system is prepared initially in a partially entangled state is much better than that if we start with a charged qubit in an excited state (product state). The effect of the mean photon number is seen if we take a look at Fig.(7b), where we consider $\bar{n} = 10$. From this figure, we can see that the Rabi oscillations shrunk and shifted to the right as time increases. Due to the shrunk of the oscillations, we can see that the channel capacity increases a little bit as \bar{n} increases. From Fig.(4b) and Fig.(7b), we can see that there is a strong relation between the degree of entanglement and the channel capacity and hence the rate of transform data. This maximum value of the channel capacity is obtained at a large degree of entanglement, as an example in the interval $[0.2, 0.8]$. Also, from equation (10), the capacity of the channel does not

only depend on the channel ρ_{ab} , but also on the individual state for the single qubit ρ_b . It is clear on the interval [10-20] as an example, the degree of entanglement is almost zero, but the capacity does not vanish.

6 Conclusion

In this paper we have studied in a non-standard way the dynamics of the Bloch vectors for two charged qubits. We investigate the dynamical behavior of the Bloch vector for each qubit. The shrunk, extension and the direction of these vectors are examined for different parameters of the charged system and the cavity field. We show for strong coupling between the filed and the charged system, the Bloch vector for the two qubits have the same behavior. But if one qubit has a weak coupling with the field (as the second qubit in our case), the behavior of the two Bloch vectors is different.

Using the density matrix technique, we predict the existence of entangled states, where we consider an entanglement measure which depends on the two Bloch vectors and the cross dyadic and is called entangled dyadic. The relation between the evolvment of the Bloch vector and the degree of entanglement is shown, where for large values of the Bloch vectors, the degree of entanglement is minimum. It is shown that, for a charged qubit prepared initially in an entangled state, the amount of entanglement is much larger than that for any other choices. The role played

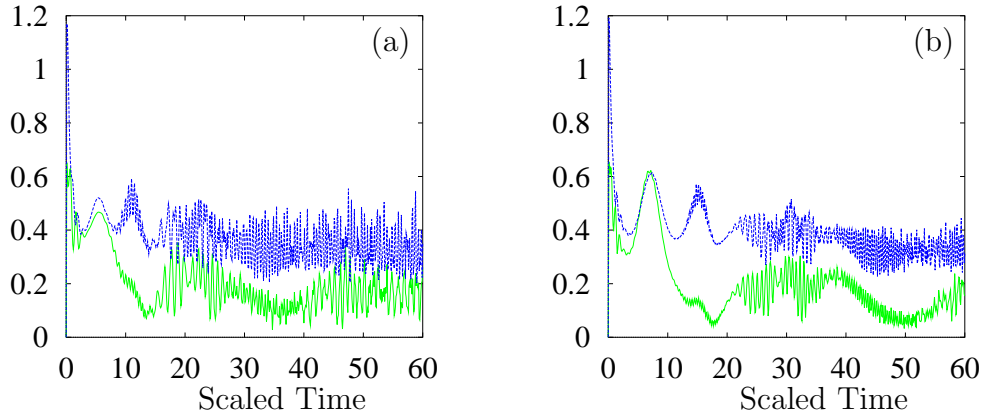


Figure 7: The capacity of the channel where $R = 0.9$ The solid and dot curves for a charged system is prepared initially in a partially entangled and excited states respectively. (a) for $\bar{n} = 10$, and (b) For $\bar{n} = 20$.

by the coupling constant and the mean photon number is cleared for generating entangled states and improving its degree of entanglement. Decreasing the mean photon number of the cavity mode is important to generate entangled state even the coupling between the qubits and field is weak.

The behavior of the channel capacity between the two charged qubits is examined, using different regimes of preparing the initial state of the system. It is shown that the possibility of generating entangled state with high capacity and consequently high rate of transmission of information is much better if we start with a partially entangled state for the system. Also, the mean photon number plays a central role in the efficient of the channel capacity, where for small values of the mean photon numbers, the channel capacity is increased and consequently the transmission rate of information.

References

- [1] D. P. DiVincenzo, *Science*, **270** 255, (1995); A. K. Ekert and R. Jozsa, *Rev. Mod. Phys.* **68** 733 (1996).
- [2] A. K. Ekert, *Phys. Rev. Lett.* **67** 661, (1991).
- [3] C. H. Bennett, G. Brassard, C. Crepeau, R. Jozsa, A. Peres and W. K. Wootters, *Phys. Rev. Lett* **70** 1895 (1993).
- [4] C. H. Bennett and S. J. Wiesner *Phys. Rev. Lett.* **69** 2881 (1993).
- [5] X. San Ma and A. Min Wang, *Opt. Commun.* **270** 465 (2007).
- [6] M. Zhang, J. Zpu and B. Shao, *Int. J. Mod. Phys. B* **16** 4767 (2002), W. Krech and T. Wanger, *Phys. Lett A* **275** 159 (2000), H. S. Ding, S. P. Zhao, G. H. Chen and Q. S. Yang, *Physica C* **382** 431 (2002).
- [7] Yu. Makhlin, G. Schön and A. Shnirman, *Nature* **398** 305 (1999); G. Schön, Yu. Makhlin and A. Shnirman, *Physica C* **352** 113(2001); J. Q. You and F. Nori, *Physica E* **18** 33 (2003).
- [8] G. Wendin, *R. Soc. Lond. A* **361** 1323 (2003), A. Niskanen, J. Vartiainen, and M. Salomaa, *Phys. Rev. Lett.* **90** 197901 (2003).

- [9] J. Vartiainen, A. O. Niska, M. Nakahara and M. Salomaa. Phys. Rev. A **70** 012319 (2004).
- [10] R. Fazio, J. Siewert, J. Mod . Opt.**49** 1245 (200), N. Schuch, J. Siewert, physica status solidi **233** 482 (2002).
- [11] X.-Hu Zheng, D. Pin, Yu. Zheng Xue, and CAO Zhuo-Liang; Physica C. **453** 76 (2007).
- [12] K. Tordrup and K. Molmer Phys. Rev. A**77**, 020301(R) (2008).
- [13] S. G. Schirmer, D. K. L. Oi, and A. D. Greentree, Phys. Rev. A **71** 012325 (2005).
- [14] J. Q. You, F. Nori, Physica E **18** 33 (2003). M. Paternostro¹, G. Falci, M. Kim, and G. Palma, Phys. Rev. B **69**, 214502 (2004).
- [15] D. A. Rodrigues, C. E. A. Jarvis, B. L. Gyurffy, T. P. Spiller, J. F. Annett J. Phys.: Condens. Matter, **20** 075211 (2008).
- [16] D. A. Rodrigues, T. P. Spiller, J. F. Annett, B. L. Gyurffy, J. Phys.: Condens. Matter **19** 436211 (2007).
- [17] M. Abdel-Aty, Laser Phys., **16** 1356 (2006); M. Abdel Aty, H. Abdel-Hameed and N. Metwally, Phycica C **452** 29 (2007).
- [18] L. Jak´obczyk, M. Siennicki, Phys. Lett. A 286 (2001) 383; G. Kimura, Phys. Lett. A 314, 339 (2003).
- [19] B.-G. Englert, P. Lougovski and E. Solano, Laser Phys. **13** 355 (2003).
- [20] S. Bose, V. Vedral and P.L. Knight, Phys. Rev. A **57**, 822 (1998); G. Bowen, Phys. Rev. A **63**, 022303 (2001); X. S. Liu, G.L. Long, D. M. Tong, F. Li, Phys. Rev. A **65**, 022304 (2002).
- [21] Qiu-Bo Fan and S. Zhang, Phys. Lett A **348** 160 (2006); T. Vertesi, Phys. Lett. A **357**(167) (2006).